



**HAL**  
open science

## High $^3\text{He}/^4\text{He}$ ratios in peridotite xenoliths from SW Japan revisited: Evidence for cosmogenic $^3\text{He}$ released by vacuum crushing

Reika Yokochi, Bernard Marty, Raphaël. Pik, Pete Burnard

### ► To cite this version:

Reika Yokochi, Bernard Marty, Raphaël. Pik, Pete Burnard. High  $^3\text{He}/^4\text{He}$  ratios in peridotite xenoliths from SW Japan revisited: Evidence for cosmogenic  $^3\text{He}$  released by vacuum crushing. *Geochemistry, Geophysics, Geosystems*, 2005, 6, 10.1029/2004GC000836 . insu-03619222

**HAL Id: insu-03619222**

**<https://insu.hal.science/insu-03619222>**

Submitted on 25 Mar 2022

**HAL** is a multi-disciplinary open access archive for the deposit and dissemination of scientific research documents, whether they are published or not. The documents may come from teaching and research institutions in France or abroad, or from public or private research centers.

L'archive ouverte pluridisciplinaire **HAL**, est destinée au dépôt et à la diffusion de documents scientifiques de niveau recherche, publiés ou non, émanant des établissements d'enseignement et de recherche français ou étrangers, des laboratoires publics ou privés.

Copyright



# High $^3\text{He}/^4\text{He}$ ratios in peridotite xenoliths from SW Japan revisited: Evidence for cosmogenic $^3\text{He}$ released by vacuum crushing

**Reika Yokochi**

*Centre de Recherches Pétrographiques et Géochimiques, 15 Rue Notre Dame des Pauvres, 54501 Vandoeuvre-Lès-Nancy Cedex, France (yokochi@crpg.cnrs-nancy.fr)*

**Bernard Marty**

*Centre de Recherches Pétrographiques et Géochimiques, 15 Rue Notre Dame des Pauvres, 54501 Vandoeuvre-Lès-Nancy Cedex, France*

*Also at Ecole Nationale Supérieure de Géologie, ENSG, Rue du Doyen Marcel Roubault, BP 40, 54501 Vandoeuvre-Lès-Nancy Cedex, France.*

**Raphaël Pik and Pete Burnard**

*Centre de Recherches Pétrographiques et Géochimiques, 15 Rue Notre Dame des Pauvres, 54501 Vandoeuvre-Lès-Nancy Cedex, France*

[1] In isotope studies of magmatic systems, magmatic He is preferentially extracted by crushing minerals under vacuum, whereas cosmogenic and/or radiogenic He isotopes are released by mineral melting as they are produced and remain in the mineral's matrix. Interpretation of magma source composition or surface residence time depends on the assumption that vacuum crushing releases insignificant cosmogenic  $^3\text{He}$ . We reinvestigated the helium isotopic composition of olivines in xenoliths from Takashima and Kurose volcanoes, Japan, which were reported to have high  $^3\text{He}/^4\text{He}$ , interpreted as mantle plume contributions [Sumino *et al.*, 2000; Ikeda *et al.*, 2001]. Combining vacuum crushing and heating protocols, we show that samples from both localities contain considerable concentrations of cosmogenic  $^3\text{He}$ . Significantly, up to 25% of the matrix-sited helium was extracted by prolonged crushing. It seems possible that previous high  $^3\text{He}/^4\text{He}$  ratios measured in samples from Kurose and Takashima were the result of the high cosmogenic  $^3\text{He}$  concentrations, and do not imply a mantle plume beneath Japan. For Kurose lavas sampled about 1 m above present-day sea level, exposure ages computed from cosmogenic  $^3\text{He}$  accumulation are similar to K-Ar eruption ages of  $1.13 \pm 0.12$  Ma, implying that erosion of the sampling site has been limited and that the samples have not been below sea level for prolonged periods during the last Myr. Helium extraction from the matrix by crushing cannot be explained by volume diffusion because the diffusivity of helium in olivine is slow at the crushing temperature and therefore requires an additional mechanism to enhance the release. A fracture-related extraction mechanism may be responsible for this phenomenon, and a semiquantitative model is developed assuming that the increase in specific surface area during crushing represents newly created fractures. According to this model, He released from about 10 unit cells of olivine from the fracture results in helium extraction of only 1%, but the spallation damage tracks along fractures may provide sufficient pathway for observed helium extraction of up to 25%.

**Components:** 6644 words, 9 figures, 2 tables.

**Keywords:** cosmogenic  $^3\text{He}$ ; plume; SW Japan.

**Index Terms:** 1194 Geochronology: Instruments and techniques; 1150 Geochronology: Cosmogenic-nuclide exposure dating (4918); 8121 Tectonophysics: Dynamics: convection currents, and mantle plumes.

**Received** 2 September 2004; **Revised** 13 November 2004; **Accepted** 7 December 2004; **Published** 21 January 2005.

Yokochi, R., B. Marty, R. Pik, and P. Burnard (2005), High <sup>3</sup>He/<sup>4</sup>He ratios in peridotite xenoliths from SW Japan revisited: Evidence for cosmogenic <sup>3</sup>He released by vacuum crushing, *Geochem. Geophys. Geosyst.*, 6, Q01004, doi:10.1029/2004GC000836.

## 1. Introduction

[2] Helium is a useful tracer of multiple geochemical processes. The Earth's mantle is enriched in <sup>3</sup>He relative to atmospheric and crustal helium, due to the occurrence of primordial helium trapped at the time of terrestrial accretion [Mamyrin *et al.*, 1969; Clarke *et al.*, 1969]. Mantle domains have been characterized by their <sup>3</sup>He/<sup>4</sup>He ratios. The mantle sampled by mid-ocean ridge basalts (MORBs) has a homogeneous <sup>3</sup>He/<sup>4</sup>He ratio of  $8 \pm 1$  Ra (where Ra is the atmospheric <sup>3</sup>He/<sup>4</sup>He ratio of  $1.4 \times 10^{-6}$ ), and island arc provinces display He isotopic ratios varying between the MORB range and a crustal end-member (<1 Ra). Mantle plume lavas are characterized by variable <sup>3</sup>He/<sup>4</sup>He ratios and often display values higher than those of MORBs, up to 32 Ra at Loihi Seamount, Hawaii [Kurz *et al.*, 1983], and 37 Ra in Iceland [Hilton *et al.*, 1999]. Such <sup>3</sup>He "enrichments" are interpreted as being due to mantle sources less degassed than those feeding MORBs, and therefore presumably located at greater depths [e.g., Graham, 2002, and references therein]. In addition, <sup>3</sup>He is produced at the Earth's surface by secondary neutrons resulting from interactions between galactic cosmic rays (GCR) and target nuclei. <sup>4</sup>He is produced by radioactive decay of U and Th. These in situ products are useful for dating geological processes, such as determination of surface exposure ages by <sup>3</sup>He [Niedermann, 2002] and for low temperature thermochronology ((U-Th)-He method) [Farley, 2002].

[3] A complication may arise, however, when multiple components (e.g., trapped magmatic gases and in situ produced <sup>3</sup>He and <sup>4</sup>He) reside within a single sample [e.g., Kurz, 1986; Gayer *et al.*, 2004]. A common way to address this problem is to use different extraction methods because the host sites of those components differ. In mantle-derived rocks and minerals, trapped magmatic He is concentrated in fluid inclusions, whereas radiogenic and cosmogenic isotopes remain close to their production sites within the matrix. Consequently, vacuum crushing of minerals preferentially releases trapped helium. With the assumption that this method releases negligible matrix-sited helium,

the <sup>3</sup>He/<sup>4</sup>He ratio obtained by crushing is thought to represent the magmatic component signature [e.g., Kurz *et al.*, 1986]. Furthermore, knowledge of this composition allows correction for trapped helium when attempting cosmogenic He dating [e.g., Kurz and Geist, 1999]. The validity of this assumption that negligible cosmogenic He is released by crushing is critical for interpreting He data from rocks. For example, the release of matrix-sited cosmogenic He during crushing might result in erroneous conclusions concerning the characteristics of magma sources. Hilton *et al.* [1993] in fact demonstrated that cosmogenic <sup>3</sup>He could be released during crushing, and step-wise crushing could be used to test the validity of the magmatic value by crushing.

[4] Sumino *et al.* [2000] and Ikeda *et al.* [2001] reported high <sup>3</sup>He/<sup>4</sup>He ratios up to 17.9 Ra and 11.9 Ra for peridotite xenoliths entrained in lavas from Takashima and Kurose, Japan, respectively. They proposed that these signatures were diagnostic of the contribution of a deep-seated plume component. Such an occurrence would have profound implications for the tectonics of the Japanese arc. Indeed, interactions between arc and plume mantle sources have only been documented in rare instances (e.g., back arc setting such as the Lau and Manus basins) [Hilton *et al.*, 2002, and references therein], where regional tectonics are complicated. Because Takashima and Kurose (Figure 1) sampling sites potentially have long histories of surface exposure (Figure 2), we have reinvestigated the helium isotopic composition of these peridotites. Using a combination of sequential vacuum crushing and heating techniques, we address the above-mentioned problem of the release of matrix-sited helium by crushing.

## 2. Samples

[5] Ultramafic xenoliths sampled by Takashima alkaline basalt consist mainly of cumulous dunite, wehrlite and clinopyroxenites, while mantle harzburgite and clinopyroxene-poor mantle lherzolite are predominant at Kurose (Figure 1) [Arai and Kobayashi, 1981]. Olivine separates of dunite xenoliths from Takashima analyzed by Sumino *et*

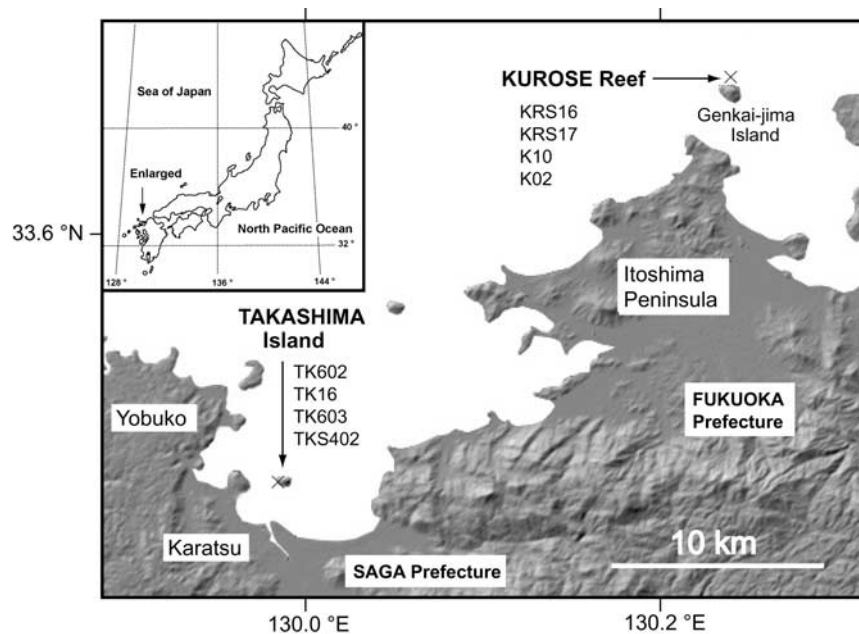


**Figure 1.** Location of Kurose and Takashima, southwest Japan. Takashima is an island located within Karatsu bay, on which dunite xenoliths were sampled at the west coast. Kurose is a reef near Genkai-jima island in Hakata bay.

*al.* [2000] yielded <sup>3</sup>He/<sup>4</sup>He ratios up to 16.6 Ra (melting extraction) and 17.9 Ra (crushing extraction), and *Ikeda et al.* [2001] reported a <sup>3</sup>He/<sup>4</sup>He ratio of 11.9 Ra (bulk melting extraction) in a harzburgite from Kurose. We analyzed olivine mineral separates from the dunites of Takashima and from the harzburgites of Kurose (Figure 1), which are likely to be similar to the samples analyzed by *Sumino et al.* [2000] and *Ikeda et al.* [2001] since the occurrences of xenolith-rich lavas are limited in size (few hundred meters long at maximum) at both localities (Figure 2).

[6] The eruption ages of the host alkaline basalts, determined by the K-Ar method, are  $3.00 \pm 0.04$  Ma for Takashima [*Nakamura et al.*, 1986], and  $1.13 \pm 0.12$  Ma for Kurose [*Uto et al.*, 1993]. Lavas containing the sampled dunite xenoliths of Takashima occur as rounded boulders that have been exposed along the coast by erosion and weathering processes (Figure 2a). No particular initial lava flow shape can be recognized for this sampling site. Analyzed dunites were sampled from different boulders, and are therefore expected to have variable exposure ages. The Kurose sampling site is a reef of several tens of meters (Fukuoka bay, Figure 2b), formed by a strongly dismantled lava flow, in which only the internal xenolith-rich columnar part is preserved. Samples have been taken in the inner part of the reef, 1 to 2 meters above the present-day maximum sea level

(Figure 2b). No exposure age is known for these two localities.

### 3. Analysis

[7] After gentle disaggregation, 0.8–3 mm olivine grains were hand-picked under a binocular microscope. Samples weighing between 0.5 g and 1.0 g were washed ultrasonically in acetone, then loaded in crushing tubes which were heated at 150°C overnight under high vacuum. Crushing was performed on-line with an iron slug activated by three external solenoids [*Richard et al.*, 1996] for variable duration (Table 1). The stroke frequency was 100/min, and the energy deposited per stroke was estimated to be 0.13 J/stroke, which results in an increase in the sample temperature of up to 50°C. Sequential crushing was prolonged in order to extract some matrix-sited component. After crushing, some of the residual powders were wrapped in Mo foil, loaded in a resistance furnace and heated at 150°C overnight under high vacuum. Helium was extracted by heating the sample at 1650°C for 20–30 min. We checked the extraction efficiency of the procedure by repeating the heating procedure until no more helium was released.

[8] Gases were sequentially purified over three titanium sponge getters cycled between 650°C and room temperature and two activated charcoal fingers at liquid nitrogen temperature. The mass spec-

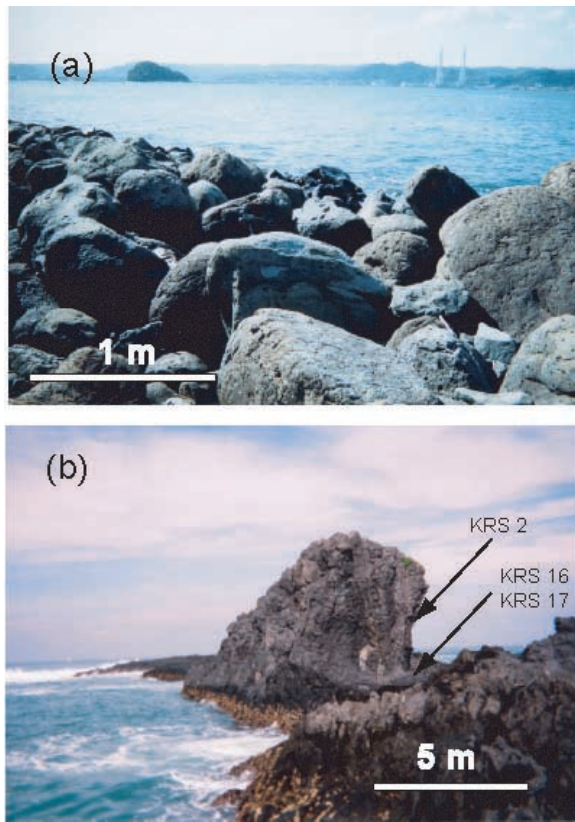


**Figure 2.** Sampling locations. (a) Located at the west coast of Takashima island, xenolith-containing boulders are abundant. Rounded boulders indicate their significant erosion history accompanying exposure. (b) Kurose, a reef in Hakata bay. Height of the reef is approximately 5 m. Lava flow was dismantled by erosion and the columnar part exposed. Duration of surface exposure, in this case, will only be the function of the erosion rate between  $\approx 1.13$  Ma (eruption age) and the present time.

trometer was optimized for the analyses of helium isotopes (Trap current: 400  $\mu$ A), and no other element was analyzed. Typical blanks for crushing and heating were  $(0.5-1.5) \times 10^{-15}$  mol <sup>4</sup>He with <sup>3</sup>He/<sup>4</sup>He = 0.06–2.4 Ra, and  $(1.0-5.9) \times 10^{-15}$  mol <sup>4</sup>He with <sup>3</sup>He/<sup>4</sup>He = 0–12 Ra, respectively. All results have been corrected for blank contributions.

## 4. Results and Discussions

### 4.1. Kurose

[9] The <sup>3</sup>He/<sup>4</sup>He ratios of Kurose samples obtained by crushing vary between 2.4 Ra up to 78.4 Ra, with many of the values above 50 Ra (Table 1, Figure 3). These values are much higher than those of Kurose reported by *Ikeda et al.* [2001] which have been interpreted as representing a mantle

plume component. They are even much higher than plume-like <sup>3</sup>He/<sup>4</sup>He ratios reported for well-known plume provinces. Indeed, the highest <sup>3</sup>He/<sup>4</sup>He ratios found in mantle plume province lavas are 37 Ra in Iceland [*Hilton et al.*, 1999] and 50 Ra in 61 Ma lavas from Baffin Island [*Stuart et al.*, 2003] associated with the onset of the plume of the North Atlantic Province. We rather propose that the extreme <sup>3</sup>He/<sup>4</sup>He ratios of this locality, Kurose, are due to the contribution of cosmogenic <sup>3</sup>He produced in the sample matrix and released during crushing. In agreement with this view, we observe that, although He isotopic compositions do not show any systematic evolution with increasing crushing steps, there is a correlation between the <sup>4</sup>He release yield (quantity of <sup>4</sup>He released/stroke) and the <sup>3</sup>He/<sup>4</sup>He ratio for the crushing data of both samples (Figure 3). This correlation is consistent with mixing between a component having a <sup>3</sup>He/<sup>4</sup>He ratio lower than the minimum observed, and a component rich in cosmogenic <sup>3</sup>He that becomes more prominent when release of the low <sup>3</sup>He/<sup>4</sup>He components is small. Thus we propose that high <sup>3</sup>He/<sup>4</sup>He ratios in Kurose ultramafic xenoliths most probably result from the contribution of cosmogenic <sup>3</sup>He produced by cosmic rays and that there is no evidence that a mantle plume contributed to volcanism in this region.

[10] The production rate of <sup>3</sup>He<sub>c</sub> in olivine, as computed with the scaling factors of *Lal* [1991], is  $100 \pm 10$  atoms/g/yr at this latitude. Assuming that all <sup>4</sup>He is from trapped helium with a <sup>3</sup>He/<sup>4</sup>He ratio of  $8 \pm 1$  Ra, the apparent exposure ages, after correction from mantle-derived <sup>3</sup>He contribution, are  $0.93 \pm 0.10$  Ma and  $1.26 \pm 0.13$  Ma, respectively, consistent with the documented eruption age of  $1.13 \pm 0.12$  Ma. This similarity supports our interpretation that the high <sup>3</sup>He/<sup>4</sup>He ratios are the result of <sup>3</sup>He produced by cosmic rays. It also suggests that the erosion of the sampling site was initially intensive (in order to expose the columnar section of the flow), and it has been limited for the rest of the 1 Myr history. Finally, this result implies that the sampling site, only about 1 m above the present-day maximum sea level, had not been significantly shielded during the last 1 Myr by sea water, with the implication that the sea level had not been significantly higher than the present level during the last 1 Myr.

### 4.2. Takashima

[11] In the case of Takashima samples, we can confirm the occurrence of <sup>3</sup>He/<sup>4</sup>He ratios up to 18.6 Ra, higher than values typical of arc magmas,

**Table 1.** Helium Isotopic Compositions and Concentrations of Olivines From Takashima and Kurose Peridotites<sup>a</sup>

Name	Run	Strokes/Temperature	$^3\text{He}/^4\text{He}$ , R/Ra	Error	$^4\text{He}$ , $10^{-14}$ mol/g	$^3\text{He}$ , $10^{-18}$ mol/g
<b><i>Takashima</i></b>						
<b>TK602b</b>						
Crushing (508 mg)	1	50	8.7	0.3	7.6	0.9
	2	100	10.0	0.4	7.6	1.1
	3	500	17.3	0.4	11.9	2.9
	4	1000	16.7	0.4	13.3	3.1
Heating (386 mg)	1	1650°C/20 min	18.6	0.4	135.5	34.9
	2	1650°C/20 min	4.9	3.7	3.5	0.2
Total			17.3		179.3	43.1
<b>TK16</b>						
Crushing (486 mg)	1	10	7.0	0.7	3.4	0.3
	2	50	8.4	0.5	5.3	0.6
	3	100	8.5	0.3	11.3	1.3
	4	500	13.9	0.4	9.2	1.8
	5	500			Lost	
	6	500	14.9	0.5	7.1	1.5
Heating (297 mg)	1	1650°C/20 min	3.0	0.11	208.4	8.6
	2	1650°C/20 min			b.l.	
Total			4.2		244.7	14.2
<b>TK603a</b>						
Crushing (489 mg)	1	10			b.l.	
	2	50	6.5	0.2	13.6	1.2
	3	100	6.4	0.6	3.6	0.3
	4	500	7.9	0.6	3.7	0.4
Heating (416 mg)	1	1650°C/20 min	1.7	0.1	222.1	5.2
	2	1650°C/20 min			b.l.	
Total			2.1		243.0	7.1
<b>TKS402a</b>						
Crushing (505 mg)	1	100	7.4	0.2	39.6	4.1
	2	500	9.0	0.2	26.2	3.3
	3	500	6.3	0.3	9.3	0.8
<b><i>Kurose</i></b>						
<b>KRS17</b>						
Crushing (1013 mg)	1	500	38.9	0.8	13.2	7.1
	2	500	39.1	0.8	13.7	7.4
	3	500	44.5	0.9	9.8	6.0
	4	500	50.7	1.0	8.5	6.0
Heating (363 mg)	1	1650°C/20 min	58.8	1.0	271.8	221.6
	2	1650°C/20 min	4.7	0.2	89.9	5.8
	3	1650°C/20 min	13.8	7.9	5.5	1.1
Total			44.6		412.5	255.1
<b>KRS16b</b>						
Crushing (1016 mg)	1	10	71.8	4.3	1.0	1.0
	2	50	58.1	1.1	11.1	9.0
	3	100	68.3	1.4	8.7	8.2
	4	500	78.4	1.5	23.3	25.3
Heating (935 mg)	1	1670°C/30 min	60.9	1.2	158.1	133.5
	2	1670°C/20 min	b.l.		b.l.	

**Table 1.** (continued)

Name	Run	Strokes/Temperature	<sup>3</sup> He/ <sup>4</sup> He, R/Ra	Error	<sup>4</sup> He, 10 <sup>-14</sup> mol/g	<sup>3</sup> He, 10 <sup>-18</sup> mol/g
Total			63.1		202.1	176.9
<b>K10</b>						
Crushing (529 mg)	1	50			0.2	
	2	100			0.5	
	3	500	2.4	0.9	2.0	0.1
<b>K02</b>						
Crushing (502 mg)	1	50	47.3	3.8	1.5	1.0
	2	100	47.0	1.5	4.8	3.1
	3	500	54.8	1.1	17.7	13.4

<sup>a</sup> Errors are at 1σ.

which could be diagnostic of the contribution of plume-related magmas. However, the release patterns of <sup>3</sup>He/<sup>4</sup>He ratios with crushing rather suggest the occurrence of cosmogenic <sup>3</sup>He<sub>c</sub> in these samples as well. All samples show comparatively low <sup>3</sup>He/<sup>4</sup>He ratios (between 6.5 and 8.7 Ra) during the first crushing steps. These values are typical of arc magmas in general, and Japan in particular [e.g., Sano *et al.*, 1984]. Higher ratios are observed as crushing proceeds, and the highest value is found during the heating experiment of sample TK602b (18.6 Ra). Such release behavior is typical of samples having trapped magmatic helium in fluid inclusions and having accumulated <sup>3</sup>He<sub>c</sub> in their matrix [e.g., Hilton *et al.*, 1993; Stuart *et al.*, 1994; Scarsi, 2000].

[12] The release pattern of helium from sample TK602b, which provides the best example for the occurrence of <sup>3</sup>He<sub>c</sub>, indicates that ≈8% of <sup>3</sup>He<sub>c</sub> is released during the last crushing steps (Figure 4; 500 and 1,000 strokes). These <sup>3</sup>He/<sup>4</sup>He ratios are comparable to those observed during heating of the powder. Samples TK603a and TKS402a do not show evidence for <sup>3</sup>He<sub>c</sub> by crushing as the He isotope data are compatible with release of trapped magmatic helium. Radiogenic He is released during heating of TK603a (Table 1) which is probably related to in situ U and Th decay. Sample TK16 has a somewhat complicated release pattern. The <sup>3</sup>He/<sup>4</sup>He ratios increase regularly with crushing from an arc-type value of 7–8.5 Ra to 14 Ra (500 strokes), and then decrease toward a more radiogenic value of 3.0 Ra during the heating experiment. Differences in the He isotopic ratios between crushing and heating requires an additional source of <sup>4</sup>He which is only released by heating and not by extensive crushing. Selective release of this more radiogenic component by heating indicates that this component does not reside homogeneously in the matrix and has different sites than cosmogenic

<sup>3</sup>He. Obvious candidates for such sites are melt or mineral inclusions containing U, Th that were not sampled during crushing due to their small size.

[13] The maximum apparent exposure age, computed assuming a <sup>3</sup>He/<sup>4</sup>He ratio of 8 ± 1 Ra for trapped helium, is 0.14 Ma for TK602, indicating significant shielding since the time of eruption 3 Myr ago. This is consistent with typical erosion processes that have shaped the sampled boulders.

#### 4.3. Release Mechanism of Cosmogenic and Radiogenic He Isotopes

[14] Assuming that the trapped component has a He isotopic composition of 8 ± 1 Ra and that all

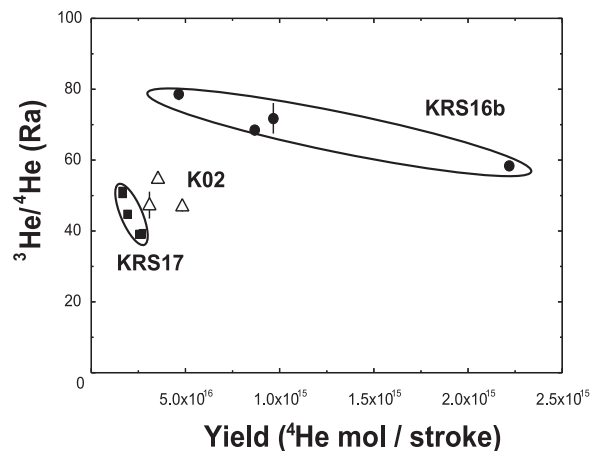


**Figure 3.** Anticorrelation between helium isotopic composition and helium yield for each sample from Kurose, implying a mixing between a trapped component having low <sup>3</sup>He/<sup>4</sup>He ratio and in situ produced cosmogenic <sup>3</sup>He<sub>c</sub>. Data from the same sample are grouped within an ellipse. K02 does not show a clear inverse correlation due to the fact that (1) the ranges of the variations in both yield and isotopic composition are small and (2) the relatively large error was assigned for the isotopic composition of the first step.

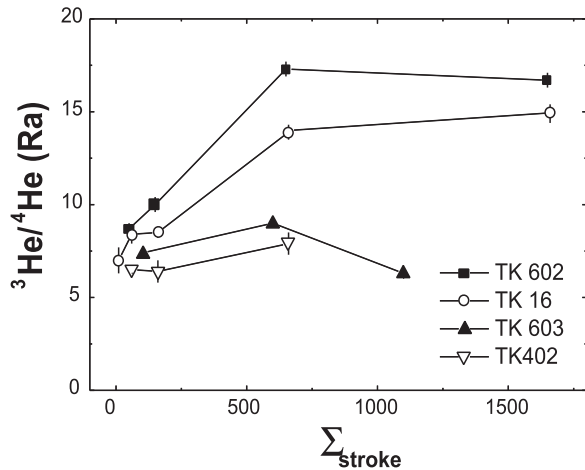


**Figure 4.** Evolution of <sup>3</sup>He/<sup>4</sup>He ratio with cumulative strokes for Takashima. Two of the samples showed significant increases in the ratio when crushing proceeds.

<sup>4</sup>He is trapped in fluid inclusions, as much as 15%, 25% and 10% of the matrix-sited <sup>3</sup>He is extracted by prolonged crushing of samples TK602b, KRS16b, KRS17, respectively. The contribution of matrix-sited He increases as crushing proceeds for samples TK16 and TK602, as independently documented in other samples [Hilton *et al.*, 1993; Scarsi, 2000]. This behavior suggests diffusion during release could play a major role. However, at the low crushing temperatures ( $\leq 50\text{C}^\circ$ ), the diffusivity of helium in olivine (extrapolated from measurements obtained at higher temperatures) would be  $\approx 2.4 \times 10^{-21} \text{ cm}^2/\text{sec}$  [Trull *et al.*, 1991]. For the duration of the experiment, the expected diffusion is by far less than the atomic radius of helium (1.78 Å for crystal [Ozima and Podosek, 2002]). Therefore solid-state volume diffusion is unlikely, and another process of He extraction is required.

[15] Helium may be extracted at the fractured surface due to lattice distortion caused by plastic deformation during fracturing. If we assume that a

certain depth from the fracture is subject to helium loss, then the volume subject to helium extraction may be estimated from (1) the size of the newly created fracture surface and (2) the depth of deformation resulting in the loss. Assuming that the area of newly created fracture surface can be represented by an increase in specific surface area (SSA), we semiquantitatively model a fracture-driven release mechanism below.

#### 4.3.1. Model

[16] Brantley and Mellott [2000] experimentally determined the relationship between SSA ( $\text{cm}^2/\text{g}$ ) and the grain radius  $r$  ( $\mu\text{m}$ ) for olivine as  $\log(\text{SSA}) = 5.2 - \log(2r)$ . In order to determine SSA of our olivines after crushing, it is thus necessary to establish their grain size distribution. Assuming that the grains are spheres and that the number of grains increases exponentially with decreasing radius ( $N(r) = ke^{-mr}$ ), the relationship between the initial (i.e., before crushing) number of grains  $N_i$  with radius  $r_i$  (mass conservation) is

$$N_i \times r_i^3 = \int_0^{r_i} N(r) \times r^3 dr. \quad (1)$$

If we consider only grains smaller than a given size ( $r < r_c$ ), the mass fraction ( $f$ ) of these crushed minerals having radii smaller than  $r_c$  is

$$f = \int_0^{r_c} N(r)r^3 dr / (N_i \times r_i^3), \quad (2)$$

which defines the size distribution curve  $N(r)$  as a function of  $N_i$ ,  $r_i$ ,  $f$  and  $r_c$ . Typical  $r_i$  in this study was between 0.4 and 1.5 mm, and was set at 1 mm. Changing this parameter within the range will not significantly affect the result as the SSA of the uncrushed grains is negligible compared to that of the crushed powders. To define the size distribution curve representing that of 1 g of material,  $N_i$  was computed for 1g of grains with  $r = r_i$ . Selection of  $r_c$  depends on the actual grain

**Table 2.** Size Distributions of the Crushed Olivine<sup>a</sup>

	Diameter					Recovered
	>600 $\mu\text{m}$	600–425 $\mu\text{m}$	425–140 $\mu\text{m}$	140–75 $\mu\text{m}$	<75 $\mu\text{m}$	
TK16	0.8%	2.3%	24.4%	19.6%	52.9%	65%
TKS402a	14.8%	10.6%	37.6%	17.2%	19.7%	92%
TK603a	2.0%	4.9%	33.3%	19.1%	40.7%	86%
TK602b	0.0%	1.2%	14.2%	18.4%	66.2%	78%
KRS17a	0.6%	3.1%	21.9%	49.8%	24.5%	72%
KRS16b	24.8%	7.8%	29.4%	16.8%	21.2%	93%

<sup>a</sup> Samples were sieved after crushing with mesh sizes of 75, 140, 425, 600  $\mu\text{m}$ . Note that size of mesh is considered to be the grain diameter in the modeling.

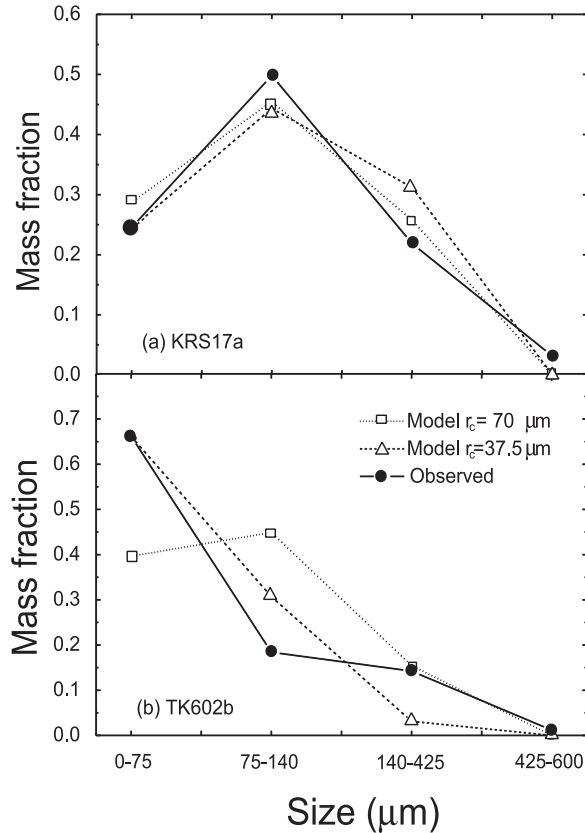


**Figure 5.** Masses of different sieved fractions of the actual crushed residue (solid circle) and that predicted by the model assuming an exponential grain size distribution (open triangle and square) using two different boundary conditions ( $r_c$ ; see text for model). Size indicates the size of mesh used for sieving. (a) KRS17 shows a nearly perfect match, indicating that the assumption for the grain size distribution calculation is appropriate for this sample, and (b) TK602b does not meet the observed distribution with either model, but provides upper and lower limits for calculation of SSA (see text).

size distribution after crushing and will be discussed later.

[17] SSA after crushing can be estimated ( $SSA_f$ ) using the computed grain size distributions:

$$SSA_f = \int_0^{r_i} N(r) \times \rho V(r) \times SSA(r) dr, \quad (3)$$

where  $\rho$  is the sample density ( $3.3 \text{ g/cm}^3$  for olivine). When the thickness of the affected layer is  $\delta l$ , the mass fraction subject to helium loss ( $R_v$ ) is approximately

$$R_v \approx SSA_f \times \delta l \times \rho. \quad (4)$$

### 4.3.2. Model Results

[18] The validity of the assumption of an exponential grain size distribution can be tested by comparing the predicted grain size distribution with the masses of different sieved fractions of the actual crushed samples, which are listed in Table 2. We define the mass fractions of 0–75  $\mu\text{m}$ , 75–140  $\mu\text{m}$ , and 140–425  $\mu\text{m}$  (mesh size) to be F1, F2, and F3, respectively. Note that the size of mesh is considered to be the grain diameter ( $2r_c$ ) in the model. Size distribution curves were calculated for  $r_c = 70 \mu\text{m}$  ( $f = F1 + F2$ ) and 37.5  $\mu\text{m}$  ( $f = F1$ ) for comparison. One sample, KRS17, showed a nearly perfect fit at both values of  $r_c$  (Figure 5a), and the exponential grain size distribution is clearly valid for this sample. Relatively well crushed samples (TK602b, TK16, TK603a) showed more complex grain size distribution relative to the models (Figure 5b). Because SSA is large for smaller grains, overestimation of the small grain size fractions causes overestimation of SSA and vice-versa. The model with  $r_c = 70 \mu\text{m}$  underestimates F1 but overestimates F2, therefore the resulting SSA must be an underestimate, i.e., this model provides the lower limit on SSA. Also shown in Figure 5b is the model with  $r_c = 37.5 \mu\text{m}$ . This curve overestimates the F2 fraction and underestimates the F3 fraction, thus the resulting SSA must be an overestimate, giving the upper limit on SSA. Thus, for these samples, we can bracket the SSA according to this diagram. A similar interpretation can be applied to the other two samples, KRS16b and TKS402a.

[19] The calculated values of  $SSA_f$  are plotted as a function of  $f$  for  $r_c = 70 \mu\text{m}$  and 37.5  $\mu\text{m}$  in Figure 6, together with that of the samples for each model. As mentioned above, the two models provide lower and upper limits. As is expected, SSA increases with  $f$  at a given  $r_c$ , and with decreasing  $r_c$  at constant  $f$  value. For well-crushed samples, SSA exceeds  $2500 \text{ cm}^2/\text{g}$ , and is between 1200 and  $1600 \text{ cm}^2/\text{g}$  for less crushed samples.

[20] The volume fraction subject to He loss ( $R_v$ ) for  $r_c = 37.5 \mu\text{m}$  is shown in Figure 7, which increases with the distance from the fracture ( $\delta l$ ) affected by He loss, and increases with  $f$ . Here, we suppose that  $\delta l$  varies by unit cells of olivine (1.02 nm). According to this calculation, it appears possible to release about 1% of the matrix sited helium when 10 unit cells of olivine from the fracture are subject to He loss. This could be a lower limit since molecular dynamics modeling

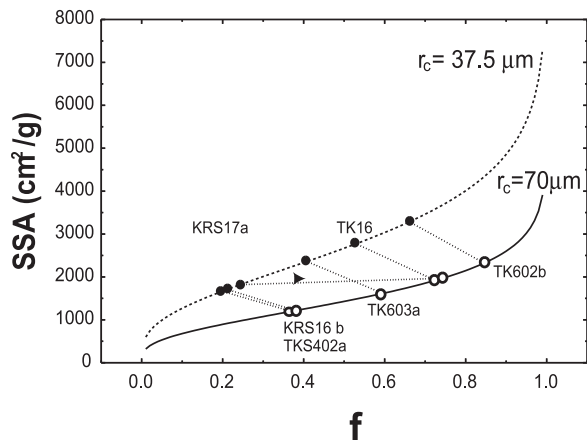


**Figure 6.** Modeled SSA at  $r_c = 37.5 \mu\text{m}$  (dotted line) and  $70 \mu\text{m}$  (solid line) as a function of  $f$  (curves). Along the model curves, SSA for each sample can be estimated according to the measured  $f$  (sieved mass fractions) at a given  $r_c$ , plotted as open circles ( $r_c = 70 \mu\text{m}$ ) and solid circles ( $r_c = 37.5 \mu\text{m}$ ) with sample names. Plots of identical sample at different  $r_c$  are tied with dotted lines. As in the text, models with  $r_c = 37.5 \mu\text{m}$  and  $70 \mu\text{m}$  give upper and lower SSA limits, respectively; thus the projection of the tie line to the y axis gives the expected range in SSA for each sample.

shows that the forces acting on the surface layers are able to lower their energy by being displaced away from their normal positions over a length scale of several unit cells below the surface. Thus this model already leads us considerably closer to the observation compared to assuming simple volume diffusion. Nevertheless, there is still about one order of magnitude gap between observed and modeled He extraction (Figure 7), implying either (1) more than 100 unit cells of olivine from the fractures are subject to He loss or (2) there is a mechanism to further induce He extraction along the fracture-related release.

[21] Defects in the minerals may induce helium loss at the fractures. TEM studies of olivine shock experiments show that dislocations at high concentration are associated with fractures, i.e., dislocations nucleate at fractures [Langenhorst *et al.*, 1999]. High dislocation densities at the fracture may facilitate the helium extraction. Another noteworthy point is that the size distribution of residual powder does not simply correlate with the degree of matrix-sited He release. For example, KRS16b released the largest proportion of matrix-sited <sup>3</sup>He<sub>c</sub> although the fraction of grains smaller than 140 μm does not reach 40%, i.e., crushing efficiency was the lowest while extraction from the matrix was the largest. Although such effect on the SSA (thus R<sub>v</sub>)

is about a factor of two at most (Figure 6), this observation implies that there is also a sample-specific parameter that controls He release, such as degree of alteration and/or the density of intrinsic defects. These parameters are at present difficult to quantify.

[22] The lattice damage generated by the spallation reactions may also induce the helium loss. Although information on the length of spallation damage tracks is scarce, a study of meteorites reported spallation damage tracks of c.a. 10 μm in olivines [Finkel *et al.*, 1978]. We may also be able to scale the results of nuclear emulsion studies: given that spallation recoil is 50 μm in emulsion (density = 1 g/cm<sup>3</sup> [Rossi, 1952]) and assuming that the scaling laws for alpha particles with density are applicable [after Ziegler, 1977], spallation track length was modeled as a function of density and is shown in Figure 8. At the density of olivine (3.3 g/cm<sup>3</sup>), the scaled curve gives the track length of 14 μm. From these two estimates, it is reasonable to consider that the spallation track length in olivine is between 10 and 15 μm.

[23] In an extreme case, each cosmogenic He atom which lies at the end of an open damage track will be released when the track encounters the fracture. Then, grains with a diameter smaller than the length of damage tracks release all cosmogenic helium. For larger grains, the half length of damage tracks should correspond to  $\delta l$  defined above. In this case, however, the volume fraction subject to He loss (R<sub>v</sub>) can not be determined by equation (4) because  $\delta l$  is not negligible relative to the size of surface irregularities, resulting in an overestimation

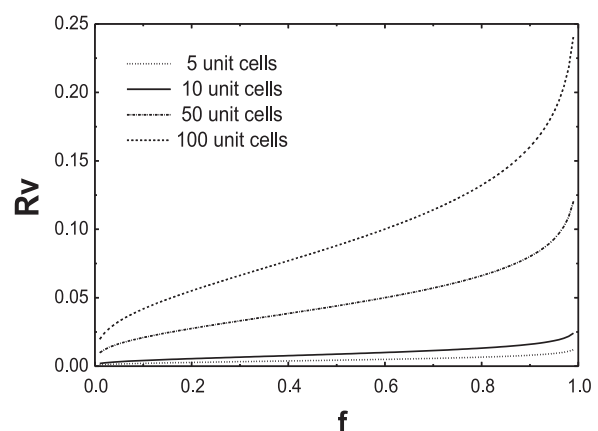


**Figure 7.** Modeled volume fraction (R<sub>v</sub>, for  $r_c = 37.5 \mu\text{m}$ ) subject to He loss, at different thickness of the affected layer from the fracture.

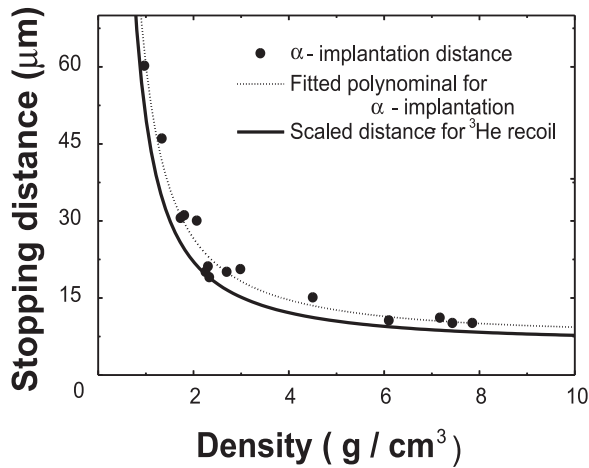


**Figure 8.** Track length versus density, estimated by scaling the spallation recoil in emulsion. Circles are alpha-implantation distance in various elements. Dotted curve represents the fit to the element data. Using the boundary condition from emulsion (50  $\mu\text{m}$  at  $1 \text{ g/cm}^3$ ), the curve was rescaled and plotted as a solid line. According to the diagram,  $^3\text{He}$  recoil length in olivine is estimated to be  $14 \mu\text{m}$ .

of  $R_v$ . Instead, we can estimate the volume fraction that retains its  $^3\text{He}$  as

$$f_s = \int_t^{r_i} N(r)(r-t)^3 dr / (N_i \times r_i^3), \quad (5)$$

where  $t$  is the length of damage tracks. This corresponds to the volume fraction keeping 100% helium. The layer below the surface within a thickness  $t$  will lose about half of the cosmogenic helium due to the fact that the orientation of tracks is random, thus 50% of the tracks will terminate in the crystal and the rest at the fracture.

[24] Supposing that (1) all helium is lost from the grains with  $2r < t$  and this volume fraction is estimated by the modeled grain size distribution (Figure 6), (2) volume fraction  $f_s$  will keep all its helium, and (3) the remaining fraction (i.e., the outer layer of thickness  $t$ ) loses half of its helium, the estimated volume fractions subject to helium loss are plotted against SSA for different spallation track length. The result of this calculation is shown in Figure 9 as a function of SSA. Over the range of SSA we estimated for our samples (1500–2500  $\text{cm}^2/\text{g}$ ), it appears possible to actually extract a few tens of percent of helium from the matrix. Note that the fraction of small grains subject to complete helium loss never exceeds 2.5% of the total mass.

[25] If the spallation damage track is actually a main controlling factor for the release of matrix-

sited helium, the method of extraction is expected to be an elementally fractionating process since the recoil length would be different for different elements. Neon isotopic composition serves as a proxy to distinguish the “primitive” and “cosmogenic” components. However, elemental fractionation that is expected to occur during the extraction may limit its quantitative use as a proxy. A study on the extraction behavior of neon relative to helium is recommended to test the sensitivity of this element to crushing, which also serves as a clue to test the release mechanism of noble gases from mineral matrices proposed herein.

[26] In one of our samples, TK16, the radiogenic component was not released by crushing. We attributed this selective extraction to a different site (melt or mineral inclusions) of the radiogenic helium than cosmogenic  $^3\text{He}$ . The idea that the damage tracks play important role for the extraction of matrix-cited helium supports the selective retention of radiogenic helium in small inclusions, having lower probability for the  $\alpha$ -damage tracks to encounter the fractures.

[27] The consequence of He extraction by crushing results in two types of misleading interpretations. A typical example of one is presented in this work: overestimation of trapped  $^3\text{He}/^4\text{He}$  ratios on samples with long exposure ages. Samples with low trapped/matrix helium contents are subject to this problem. The other consequence is the case where a combination of crushing and subsequent heating is used to distinguish trapped He from cosmogenic He in a single sample. It is generally assumed that matrix-sited helium is not released during crushing. If our observation (extraction of >10% of matrix-

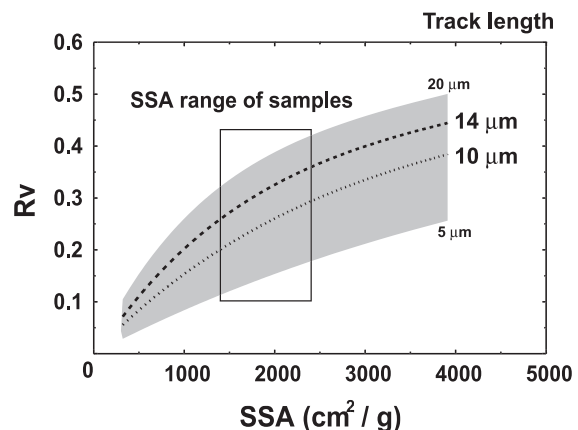


**Figure 9.** Modeled volume fraction subject to helium loss ( $R_v$ ) due to GCR damage tracks. At the observed range of SSA (in box), it appears possible to extract a few tens of % of helium from the olivine matrix.

sited He by crushing) applies, this method will underestimate the matrix-sited component. For studies requiring high precision, this point is recommended for further evaluation.

## 5. Conclusion

[28] Cosmogenic <sup>3</sup>He was observed in peridotitic xenoliths from two localities in Japan, Takashima and Kurose, where contributions from a mantle plume has previously been proposed. The contribution of a plume component was not confirmed by the present study.

[29] For Takashima, our data support the contention made by *Sumino et al.* [2000] that a trapped He component exists that has a MORB-like signature. However, it was demonstrated that <sup>3</sup>He/<sup>4</sup>He ratios higher than MORBs in this study are due to a contribution from cosmogenic <sup>3</sup>He<sub>c</sub>.

[30] For Kurose, <sup>3</sup>He/<sup>4</sup>He ratios of 11.9 Ra obtained from heating experiments were also regarded as being due to a mantle plume [*Ikeda et al.*, 2001]. These authors dismissed a cosmogenic origin for <sup>3</sup>He on the ground that their “excess” <sup>3</sup>He was too small to result from surface exposure since the time of eruption. We show that extremely high <sup>3</sup>He/<sup>4</sup>He ratios up to 78 Ra are unlikely to result from a mantle plume and that exposure ages for the samples analyzed in the present study fit K-Ar ages. The coherency between K-Ar eruption age and <sup>3</sup>He exposure age indicates that the sampling site suffered very limited erosion, and that there was no significant shielding by sea water since 1 Myr. Lower apparent exposure ages of samples from Kurose analyzed by *Ikeda et al.* [2001] are probably the result of heterogeneous shielding.

[31] Crushing releases a significant proportion (up to 25%) of He from the matrix, and the isotopic composition of gas-poor samples was significantly modified from the trapped component released by crushing. Quantitative release of matrix-sited helium cannot be explained by volume diffusion, and spallation damage tracks along fractures may provide sufficient pathway for helium extraction.

## Acknowledgments

[32] We are grateful to P-H. Blard and L. Zimmermann for their help in laboratory and to H. Sumino, E. Gayer, and N. Dauphas for discussions. M. Yokochi, Y. Watanabe, and J. Yamamoto are acknowledged for their support during sampling. Advice from M. Toplis and M. Roskosz greatly contributed to the development of the model. Advice from

R. Lewis and T. Dunai was very helpful for estimating the effect of the GCR damage track. We appreciate comments from associate editor D. Hilton and reviewers F. Stuart and M. Moreira. Particularly, the comment from F. Stuart suggesting the contribution of GCR damage led our model much closer to the observation. This is CRPG contribution 1715.

## References

- Arai, S., and Y. Kobayashi (1981), Frequency of ultramafic rocks as inclusions in some alkali basalts from southwestern Japan and its bearing on the constitution of the upper mantle, annual report, pp. 66–69, Univ. of Tsukuba, Tsukuba, Japan.
- Brantley, S. L., and N. P. Mellott (2000), Surface area and porosity of primary silicate minerals, *Am. Mineral.*, *85*, 1767–1783.
- Clarke, W. B., M. A. Beg, and H. Craig (1969), Excess <sup>3</sup>He in the sea: Evidence for terrestrial primordial helium, *Earth Planet. Sci. Lett.*, *6*, 213–220.
- Farley, K. A. (2002), (U-Th)/He dating: Techniques, calibrations, and applications, in *Noble Gases in Geochemistry and Cosmochemistry*, edited by D. Porcelli, C. J. Ballentine, and R. Wieler, *Rev. Mineral. Geochem.*, *47*, 819–844.
- Finkel, R. C., C. P. Kohl, K. Marti, and B. Martinek (1978), The cosmic ray record in the San Juan Capistrano meteorite, *Geochim. Cosmochim. Acta*, *42*, 241–250.
- Gayer, E., R. Pik, J. Lavé, C. France-Lanord, D. Bourlès, and B. Marty (2004), Cosmogenic <sup>3</sup>He in Himalayan garnets indicating an altitude dependence of the <sup>3</sup>He/<sup>10</sup>Be production ratio, *Earth Planet. Sci. Lett.*, *229*(1-2), 91–104.
- Graham, D. W. (2002), Noble gas isotope geochemistry of Mid-Ocean Ridge and Ocean Island Basalts: Characterization of Mantle Source Reservoir, in *Noble Gases in Geochemistry and Cosmochemistry*, edited by D. Porcelli, C. J. Ballentine, and R. Wieler, *Rev. Mineral. Geochem.*, *47*, 247–318.
- Hilton, D. R., K. Hammerschmidt, S. Teufel, and H. Friedrichsen (1993), Helium isotope characteristics of Andean geothermal fluids and lavas, *Earth Planet. Sci. Lett.*, *120*, 265–282.
- Hilton, D. R., K. Gronvold, C. G. Macpherson, and P. R. Castillo (1999), Extreme <sup>3</sup>He/<sup>4</sup>He ratios in northwest Iceland: Constraining the common component in mantle plume, *Earth Planet. Sci. Lett.*, *173*, 53–60.
- Hilton, D. R., T. P. Fischer, and B. Marty (2002), Noble gases and volatile recycling at subduction zones, in *Noble Gases in Geochemistry and Cosmochemistry*, edited by D. Porcelli, C. J. Ballentine, and R. Wieler, *Rev. Mineral. Geochem.*, *47*, 319–370.
- Ikeda, Y., K. Nagao, and H. Kagami (2001), Effects of recycled materials involved in a mantle source beneath the southwest Japan arc region: Evidence from noble gas, Sr, and Nd isotopic systematics, *Chem. Geol.*, *175*, 509–522.
- Kurz, M. D. (1986), Cosmogenic helium in a terrestrial igneous rock, *Nature*, *320*, 435–439.
- Kurz, M. D., and D. Geist (1999), Dynamics of the Galapagos hotspot from helium isotope geochemistry, *Geochim. Cosmochim. Acta*, *63*, 4139–4156.
- Kurz, M. D., W. J. Jenkins, S. R. Hart, and D. Clague (1983), Helium isotopic variations in volcanic rocks from Loihi Seamount and the Island of Hawaii, *Earth Planet. Sci. Lett.*, *66*, 388–406.
- Lal, D. (1991), Cosmic ray labelling of erosion surfaces: In situ nuclide production rates and erosion models, *Earth Planet. Sci. Lett.*, *104*, 424–439.

- Langenhorst, F., M. Boustie, A. Migault, and J. P. Romain (1999), Laser shock experiments with nanoseconds pulses: A new tool for the reproduction of shock defects in olivine, *Earth Planet. Sci. Lett.*, *173*, 333–342.
- Mamyrin, B. A., I. N. Tolstikhin, G. S. Anufriyev, and I. L. Kamenskiy (1969), Anomalous isotopic composition of helium in volcanic gases, *Dokl. Akad. Nauka SSSR*, *184*, 1197–1199.
- Nakamura, E., I. MacDougall, and H. I. Cambell (1986), K-Ar ages of basalts from the Higashi-Matsuura district, northwestern Kyushu, Japan and regional geochronology of the Cenozoic alkaline volcanic rocks in eastern Asia, *Geochem. J.*, *20*, 91–99.
- Niedermann, S. (2002), Cosmic-ray-produced noble gases in terrestrial rocks: Dating tools for surface processes, in *Noble Gases in Geochemistry and Cosmochemistry*, edited by D. Porcelli, C. J. Ballentine, and R. Wieler, *Rev. Mineral. Geochem.*, *47*, 731–784.
- Ozima, M., and F. Podosek (2002), *Noble Gas Geochemistry*, Cambridge Univ. Press, New York.
- Richard, D., B. Marty, M. Chaussidon, and N. Arndt (1996), Helium isotopic evidence for a lower mantle component in depleted Archean komatiite, *Science*, *273*, 93–95.
- Rossi, B. B. (1952), *High-Energy Particles*, Prentice-Hall, Upper Saddle River, N. J.
- Sano, Y., Y. Nakamura, H. Wakita, A. Urabe, and T. Tominaga (1984), Helium-3 emission related to volcanic activity, *Science*, *224*, 150–151.
- Scarsi, P. (2000), Fractional extraction of helium by crushing of olivine and clinopyroxene phenocrysts: Effects on the <sup>3</sup>He/<sup>4</sup>He measured ratio, *Geochim. Cosmochim. Acta*, *64*(21), 3751–3762.
- Stuart, F. M., G. Turner, and R. Taylor (1994), He-Ar isotope systematics of fluid inclusions: Resolving mantle and crustal contributions to hydrothermal fluids, in *Noble Gas Geochemistry and Cosmochemistry*, edited by J. Matsuda, pp. 261–277, Terra Sci., Tokyo.
- Stuart, F. M., S. Lass-Evans, J. G. Fitton, and R. M. Ellam (2003), High <sup>3</sup>He/<sup>4</sup>He ratios in picritic basalts from Baffin Island and the role of a mixed reservoir in mantle plumes, *Nature*, *424*, 57–59.
- Sumino, H., S. Nakai, K. Nagao, and K. Notsu (2000), High <sup>3</sup>He/<sup>4</sup>He ratio in xenoliths from Takashima: Evidence for plume type volcanism in southwestern Japan, *Geophys. Res. Lett.*, *27*(8), 1211–1214.
- Trull, T. W., M. D. Kurz, and W. J. Jenkins (1991), Diffusion of cosmogenic <sup>3</sup>He in olivine and quartz: Implications for surface dating, *Earth Planet. Sci. Lett.*, *103*, 241–256.
- Uto, K., H. Hirai, and S. Arai (1993), K-Ar ages for Quaternary alkali basalts from Kurose, Fukuoka Prefecture and Kifune, Yamaguchi Prefecture, Southwest Japan, *Bull. Geol. Surv. Jpn.*, *44*(11), 693–698.
- Ziegler, J. F. (1977), *Helium: Stopping Powers and Ranges in all Elemental Matter*, vol. 4, *The Stopping and Ranges of Ions in Matter*, Elsevier, New York.